する部位に挿入したプラスミドを作成し、293T 細胞に導入して発現させたところ、それぞれエピトープ配列が挿入された SVP は培養上清中に分泌される事を確認した。

4. ウイルス粒子と抗体の反応

分泌された粒子上のエピトープに対する抗 E1 マウスモノクローナル抗体の反応性を調べたところ、遺伝子型 2a の E1 中和エピトープ挿入粒子には抗体は結合しなかったが、遺伝子型 1b の E1 中和エピトープ挿入粒子には結合することを確認した。

5. HCV 中和エピトープを持つ SVP を分泌する細胞株の樹立と粒子の精製

HCV の E1 中和エピトープ配列を挿入した JEV SVP を高発現する 293T 細胞株をレトロウイルスベクターを用いて樹立した。この細胞株の無血清培地の培養上清約 200ml から限外ろ過およびゲル濾過クロマトグラフィーを用いてウイルス粒子の精製を行い、最終的に約 700μg の精製 SVP が得られた。

6. ウイルス粒子の免疫

精製した粒子をアジュバントとともにマウス腹腔内への免疫を開始した。2 週おきに計 3 回免疫した後に、血清の中和活性を評価する。

D. 考察

HCV 中和エピトープ解析については E2 蛋白質について多く報告されているものの、E1 蛋白質の中和エピトープについては報告が少なく、我々が同定したエピトープ領域については未報告である。E1 蛋白質の HCV の感染初期過程における役割を明らかにする上でも、本結果は興味深い。

また、このエピトープに反応する抗体を効率良く誘導する抗原を調製する為に、中和エピトープ配列を持ったフラビウイルス粒子を 293T 細胞で発現させ、粒子の培養上清への分泌を確認した。中和活性を示したモノクローナル抗体は、遺伝子型 2a 由来の配列を挿入した粒子には結合しなかったものの、遺伝子型 1b 由来の配列を挿入した粒子には結合した事から、少なくとも遺伝子型 1b のエピトープ配列は粒子の外側に露出していると考えらえた。オーバーラッピングペプチドを用いたエピトープ解析では、用いた抗 E1 抗体は遺伝子型 2a 由来のペプチド配列にも強く結合が認められたため、1b と 2a の若干のアミノ酸配列の違いが粒子表面のペプチドの構造を変化させている可能性が考えられた。

現在、この抗原を精製してマウスに免疫しており、今後は中和活性を持つ抗体が誘導できるかどうかを評価する。

E. 結論

適切な HCV の中和抗体の評価が可能な 1 回感染性トランスパッケージング型 HCV 粒子(HCVtcp)産生系を用い、幅広い遺伝子型の HCV に対して中和活性を有する抗 E1 モノクローナル抗体を見いだした。この抗体のエピトープ領域を同定し、さらに遺伝子型 1b および 2a 由来のこのエピトープ配列を有する JEV SVP の産生に成功した。少なくとも遺伝子型 1b のエピトープを有する粒子については、エピトープ配列を粒子の外側に露出していると考えられ、抗体を誘導するワクチン抗原として期待できる。

F. 研究発表

1. 論文発表

1) Tanida I, Shirasago Y, Suzuki R, Abe R, Wakita T, Hanada K, Fukasawa M. Caffeic acid, a coffee-related organic acid, inhibits the propagation of hepatitis C virus. Jpn J Infect Dis. (2015) in press.

2) Tsukuda S, Watashi K, Iwamoto M, Suzuki R, Aizaki H, Okada M, Sugiyama M, Kojima S, Tanaka Y, Mizokami M, Li J, Tong S, Wakita T. Dysregulation of Retinoic Acid Receptor Diminishes

Hepatocyte Permissiveness to Hepatitis B Virus Infection through Modulation of NTCP Expression. J Biol Chem. (2015) in press.

3) Matsuda M, Suzuki R, Kataoka C, Watashi K, Aizaki H, Kato N, Matsuura Y, Suzuki T, Wakita T. Alternative endocytosis pathway for productive entry of hepatitis C virus. J Gen Virol. 95:2658-2667 (2014).
4) Yamanaka A, Suzuki R, Konishi E. Evaluation of single-round infectious, chimeric dengue type 1 virus as an antigen for dengue functional antibody assays. Vaccine. 32:4289-4295 (2014).
5) Sugiyama N, Murayama A, Suzuki R, Watanabe N, Shiina M, Liang TJ, Wakita T, Kato T. Single strain isolation method for cell culture-adapted hepatitis C virus by end-point dilution and infection. PLoS One. 9(5):e98168 (2014).

2.学会発表

1) Tsukuda S, Watashi K, Iwamoto M, Suzuki R, Aizaki H, Kojima S, Sugiyama M, Tanaka Y, Mizokami M, Wakita T. Retinoic acid receptor plays an important role in mediating hepatitis B virus infection through regulation of NTCP expression. The 11th JSH Single Topic Conference, Hiroshima, Nov, 2014
2) 史国利、安東友美、鈴木亮介、松田麻未、伊藤昌彦、中島謙治、脇田隆字、鈴木哲朗。3'UTR of HCV genome functioned as a cis-acting packaging signal. 第62回日本ウイルス学会学術集会、横浜、2014年11月
3) 大橋啓史、渡士幸一、中嶋翔、金ソルイ、鈴木亮介、相崎英樹、紙透伸治、菅原二三男、脇田隆字。Aryl hydrocarbon receptor による脂肪滴形成及び C 型肝炎ウイルス粒子構築の制御。第62回日本ウイルス学会学術集会、横浜、2014年11月
4) Lingbao Kong、青柳春代、松田麻未、藤本陽、渡士幸一、鈴木亮介、山越智、堂前直、鈴木健裕、鈴木哲朗、脇田隆字、相崎英樹。Prolactin regulatory element binding protein is involved in hepatitis C virus replication by interacting with NS4B. 第62回日本ウイルス学会学術集会、横浜、2014年11月
5) 伊藤昌彦、福原崇介、鈴木亮介、田川陽一、松浦善治、脇田隆字、鈴木哲朗。HuH-7 由来オーバル細胞様細胞株 Hdo による HCV 生活環の調節に関わる分化関連宿主因子の同定。第62回日本ウイルス学会学術集会、横浜、2014年11月
6) 中嶋翔、渡士幸一、紙透伸治、竹本健二、Jesus Izaguirre-Carbonell、鈴木亮介、相崎英樹、菅原二三男、脇田隆字。天然有機化合物 Neoechinulin B を利用した liver X receptor によるC 型肝炎ウイルス産生制御機構の解析。第62回日本ウイルス学会学術集会、横浜、2014年11月
7) 岩本将士、渡士幸一、杉山真也、鈴木亮介、相崎英樹、田中靖人、溝上雅史、大谷直子、小祝修、脇田隆字。効率的な B 型肝炎ウイルス（HBV）複製評価系を用いた微小管依存的な HBV 複製機構の解析。第62回日本ウイルス学会学術集会、横浜、2014年11月
8) 九十田千子、渡士幸一、岩本将士、鈴木亮介、相崎英樹、小嶋聡一、杉山 真也、田中靖人、溝上雅史、脇田隆字。レチノイド阻害剤は NTCP 発現修飾を介して宿主細胞の B 型肝炎ウイルス感染感受性を消失させる。第62回日本ウイルス学会学術集会、横浜、2014年11月

9) 松田麻未、鈴木亮介、嵯峨涼平、藤本陽、渡士幸一、相崎英樹、森石恆司、岡本 徹、松浦善治、黒田俊一、脇田隆字。遺伝子組換え酵母由来 B 型肝炎ウイルス様粒子の細胞表面への結合に関与する宿主因子の解析。第62回日本ウイルス学会学術集会、横浜、2014年11月

10) 渡士幸一、Sluder Ann、松永智子、梁明秀、森下了、岩本将士、九十田千子、鈴木亮介、相崎英樹、Borroto-Esoda Katyna、田中靖人、楠原洋之、杉山真也、溝上雅史、脇田隆字。B 型肝炎ウイルス（HBV）large S タンパク質と NTCP の相互作用阻害による抗 HBV 戦略。第62回日本ウイルス学会学術集会、横浜、2014年11月

11) 山中敦史、Moi MengLing、高崎智彦、倉根一郎、鈴木亮介、小西英二. デング1型ウイルスの遺伝子型がヒトにおける中和・増強抗体応答に及ぼす影響。第62回日本ウイルス学会学術集会、横浜、2014年11月

12) 嵯峨涼平、藤本陽、渡邉則幸、松田麻未、長谷川慎、渡士幸一、相崎英樹、中村紀子、小西英二、加藤孝宣、田島茂、高崎智彦、竹山春子、脇田隆字、鈴木亮介。日本脳炎ウイルスおよび C 型肝炎ウイルス 2 価ワクチン抗原の発現と中和抗体の誘導。第62回日本ウイルス学会学術集会、横浜、2014年11月

13) Saga R, Fujimoto A, Watanabe N, Matsuda M, Suzuki R, Hasegawa M, Watashi K, Aizaki H, Nakamura N, Konishi E, Kato T, Takeyama H, Wakita T. Japanese encephalitis virus-subviral particles harboring HCV neutralization epitopes induce neutralizing antibodies against HCV. 21st International Symposium on Hepatitis C Virus and Related Viruses, Banff, Canada, Sep, 2014

14) Suzuki R, Saito K, Matsuda M, Sato M, Kanegae Y, Watashi K, Aizaki H, Chiba J, Saito I, Wakita T, Suzuki T. Single domain intrabodies against HCV core inhibit viral propagation and core-induced NF-kB activation. 21st International Symposium on Hepatitis C Virus and Related Viruses, Banff, Canada, Sep, 2014

15) Fujimoto A, Aizaki H, Matsuda M, Watanabe N, Watashi K, Suzuki R, Suzuki T, Wakita T. Maintenance of HCV infectivity by down-regulating hepatic lipase expression. 21st International Symposium on Hepatitis C Virus and Related Viruses, Banff, Canada, Sep, 2014

16) Goto K, Fujimoto A, Watashi K, Suzuki R, Yamagoe S, Moriya K, Yotsuyanagi H, Koike K, Suzuki T, Wakita T, Aizaki H. NS5A-associated membrane protein, embryonic lethal, abnormal vision, drosophila-like 1, regulates hepatitis C virus RNA synthesis and translation. 21st International Symposium on Hepatitis C Virus and Related Viruses, Banff, Canada, Sep, 2014

17) Shi G, Ando, Suzuki R, Ito M, Nakashima K, Wakita T, Suzuki T. HCV 3'UTR as a cis-acting element required for the viral RNA encapsidation. 21st International Symposium on Hepatitis C Virus and Related Viruses, Banff, Canada, Sep, 2014

18) Ohashi H, Watashi K, Nakajima S, Kim S, Suzuki R, Aizaki H, Kamisuki S, Sugawara F, Wakita T. Flutamide Inhibits Hepatitis C Virus Assembly through Disrupting Lipid Droplets. 21st International Symposium on Hepatitis C Virus and Related Viruses, Banff, Canada, Sep, 2014

19) Ito M, Fukuhara T, Suzuki R, Matsuura Y, Wakita T, Suzuki T. Use of HuH7-derived, Bidirectional Oval-like cells to identify

differentiation-dependent host factors that are involved in regulation of HCV lifecycle. 21st International Symposium on Hepatitis C Virus and Related Viruses, Banff, Canada, Sep, 2014

20) Nakajima S, Watashi K, Kamisuki S, Takemoto K, Suzuki R, Aizaki H, Sugawara F, Wakita T. Regulation of hepatitis C virus replication by liver X receptor is disrupted by a fungi-derived neoechinulin B. 21st International Symposium on Hepatitis C Virus and Related Viruses, Banff, Canada, Sep, 2014

21) Watashi K, Iwamoto M, Sluder A, Matsunaga S, Ryo A, Morishita R, Kwon ATJ, Suzuki H, Tsukuda S, Suzuki R, Aizaki H, Borroto-Esoda K, Sugiyama M, Tanaka Y, Mizokamai M, Wakita T. Characterization of a culture system reproducing the NTCP-mediated HBV entry and ITS application to drug development. 2014 International Meeting on Molecular Biology of Hepatitis B Viruses, Los Angeles, USA, Sep, 2014

22) Iwamoto M, Watashi K, Sugiyama M, Suzuki R, Aizaki H, Tanaka Y, Mizokami M, Ohtani N, Koiwai O, Wakita T. Microtubule-dependent hepatitis B virus (HBV) replication revealed by chemical screening on an efficient HBV-replicating cell line. 2014 International Meeting on the Molecular Biology of Hepatitis B Viruses, Los Angeles, USA, Sep, 2014

23) Tsukuda S, Watashi K, Iwamoto M, Suzuki R, Aizaki H, Kojima S, Sugiyama M, Tanaka Y, Mizokami M, Wakita T. Retinoid inhibitors abolish the host permissiveness to HBV infection by modulating NTCP expression. 2014 International Meeting on Molecular Biology of Hepatitis B Viruses, Los Angeles, USA, Sep, 2014

24) Tsukuda S, Watashi K, Iwamoto M, Suzuki R, Aizaki H, Kojima S, Wakita T. Retinoic acid receptor regulates the expression of NTCP transporter and plays an important role in mediating hepatitis B virus infection. FASEB 2nd International Conference on Retinoids. Itasca, USA, 2014.6.1-6.

25) 青柳東代、相崎英樹、藤本陽、松本喜弘、松田麻未、Su Su Hmwe、渡邉則幸、渡士幸一、鈴木亮介、市野瀬志津子、松浦知和、鈴木哲朗、和氣健二郎、脇田隆字。グリチルリチンによる抗HCV作用 - phospholipase A2およびAutophagyによるC型肝炎ウイルス(HCV)分泌過程に与える影響 -。第24回抗ウイルス療法研究会総会、富士吉田市、2014年5月

26) 渡士幸一、Ann Sluder、松永智子、梁明秀、森下了、岩本将士、九十田千子、鈴木亮介、相崎英樹、Katyna Borroto-Esoda、田中靖人、楠原洋之、杉山真也、溝上雅史、脇田隆字。B型肝炎ウイルス(HBV)Lタンパク質とNTCPの相互作用阻害による抗HBV戦略。第24回抗ウイルス療法研究会総会、富士吉田市、2014年5月

27) 大橋啓史、渡士幸一、中嶋翔、金ソルイ、鈴木亮介、相崎英樹、紙透伸治、菅原二三男、脇田隆字。C型肝炎ウイルス粒子の構築を阻害するflutamideの作用機序の解析。第24回抗ウイルス療法研究会総会、富士吉田市、2014年5月

28) 九十田千子、渡士幸一、岩本将士、鈴木亮介、相崎英樹、小嶋聡一、脇田隆字。HBV感染受容体NTCPの発現調節機構の解析およびこれを阻害する低分子化合物の抗HBV効果。第24回抗ウイルス療法研究会総会、富士吉田市、2014年5月

29) 青柳東代、相崎英樹、松本喜弘、鈴木亮介、渡士幸一、市野瀬志津子、松浦

知和、鈴木哲朗、和氣健二郎、脇田隆字。グリチルリチンによる抗C型肝炎ウイルス作用 - phospholipase A2およびAutophagyによるHCV分泌過程の制御 - 。第50回日本肝臓学会総会、東京、2014年5月

30) 岩本将士、渡士幸一、九十田千子、Hussein Aly、藤本陽、鈴木亮介、相崎英樹、脇田隆字、深澤征義、小祝修、楠原洋之。ヒトNTCP安定発現によるB型肝炎ウイルス(HBV)感染許容性の獲得とそれを用いたHBV侵入機構の解析。第22回肝病態生理研究会、東京、2014年5月

31) Matsuda M, Nakanishi A, Li T-C, Suzuki R, Katano H, Wakita T, Suzuki T. Selective recognition of gangliosides by human polyomaviruses: Role of GD3 and GM3 in merkel cell polyomavirus infection. 7th International conference on HPV, Polyomavirus & UV in skin cancer. Novara, Italy, 2014.4.9-12

G. 知的所有権の出願・取得状況

1. 特許取得
なし。
2. 実用新案登録
なし。
3. その他
なし。

Ⅲ．　研究成果の刊行に関する一覧表

別紙４

研究成果の刊行に関する一覧表レイアウト（参考）

雑誌

発表者氏名	論文タイトル名	発表誌名	巻号	ページ	出版年
Amako Y. et al（小原）	Hepatitis C virus attenuates mitochondrial lipid β-oxidation by down-regulating mitochondrial trifunctional protein expression.	J. Virology			in press
Sato S. et al（小原）	The RNA Sensor RIG-I Dually Functions as an Innate Sensor and Direct Antiviral Factorfor Hepatitis B Virus.	Immunity	42	123-32	2015
Ezzikouri S. et al.（小原）	Inhibitory Effects of Pycnogenol® on Hepatitis C Virus Replication.	Antiviral Research	113C	93-102	2015
Tsukiyama-Kohara K. et al.（小原）	Tupaia belangeri as anExperimental Animal Model for Viral Infection.	Experimental Animal	63	367-74	2014
Lai C-K. et al.（小原）	Nonstructural Protein 5A Is Incorporated into Hepatitis C Virus Low-Density Particle through Interaction with Core Protein and Microtubules during Intracellular Transport.	PLoS ONE	9	e99022	2014
Munakata T. et al.（小原）	Suppression of hepatitis C virus replication by cyclin-dependent kinase inhibitors.	Antiviral Research	108	79-87	2014
Arai M. et al.（小原）	Resistance to cyclosporin A derives from mutations in hepatitis C virus nonstructural proteins.	Biochem Biophys Res Commun.	448	56-62	2014

Watanabe T. et al. （小原）	In vivo therapeutic potential of Dicer-hunting siRNAs targeting infectious hepatitis C virus.	Scientific Reports	23	4:4750	2014
Kasama Y. et al. （小原）	B-cell-intrinsic Hepatitis C virus expression leads to B-cell-lymphomagenesis and induction of NF-kB signaling.	PLoSONE	9	e91373	2014
Ezzikouri S. et al. （小原）	Recent insights into hepatitis B virus-host interactions.	J Medical Virology	86	925-32	2014
Yasui F. et al. （小原）	Phagocytic cells contribute to the antibody-mediated elimination of pulmonary-infected SARS coronavirus.	Virology	454-455	157-68	2014
Ogiwara H. et al. （小原）	Histopathological evaluation of the diversity of cells susceptible to H5N1 virulent avian influenza virus.	American Journal of Pathology	184	171-83	2014
Okabayashi S. et al. （保富）	Diabetes mellitus accelerates Aβ pathology in brain accompanied by enhanced GAβ generation in nonhuman primates.	PLos One			In press
Onishi M. et al. （保富）	Hydroxypropyl-β-cyclodextrin spikes local inflammation that induces Th2 cell and Tfollicular helper cell responses to the coadministered antigen.	J.Immunol			In press

Fukuyama Y. et al. （保富）	Nanogel-based pneumococcal surface protein A nasal vaccine induces microRNA-associated Th17 cell responses with neutralizing antibodies against Streptococcus pneumonias in macaques.	Mucosal Immunology	E-pub		2015
Watanabe K. et al. （保富）	Recombinant Ag85B vaccine by taking advantage of characteristics of human parainfluenza type 2 virus vector showed Mycobacteria-specific immune responses by intranasal immunization.	Vaccine	32	1727-1735	2014
Kobiyama K. et al. （保富）	Nonagonistic Dectin-1 ligand transforms CpG into a multitask nanoparticulate TLR9 agonist.	Proc. Natl. Acad Sci.USA	111(8)	3086-3091	2014
Tsujimura Y. et al. （保富）	Effects of Mycobacteria major secretion protein, Ag85B, on allergic inflammation in the lung.	Plos One	E-pub		2014
Saito N. et al. （保富）	$CD4^+$ T cells modified by the endoribonuclease MazF are safe and can persist in SHIV-infected rhesus macaques.	Mol. Ther. Nucleic Acids	E-pub		2014
Machino-Ohtsuka T. et al. （保富）	Tenascin-C aggravates autoimmune myocarditis via dendritic cell activation and Th17 cell differentiation.	J.Am.Heart Assoc.	E-pub		2014
Ezzikouri S. et al. （小原恭子）	Inhibitory effects of Pycnogenol® on hepatitis C virus replication.	Antiviral Research	113C	93-102	2015

Tsukiyama-Kohara K. et al. （小原恭子）	Tupaia belangeri as an Experimental Animal Model for Viral Infection.	Experimental Animal	63(4)	367-74	2014
Arai M. et al. （小原恭子）	Resistance to cyclosporin A derives from mutations in hepatitis C virus nonstructural proteins.	Biochem Biophys Res Commun.	448	56-62	2014
Kasama Y. et al. （小原恭子）	B-cell-intrinsic hepatitis C virus expression leads to B-cell-lymphomagenesis and induction of NF-κB signaling.	PLoS One	9(3)	E91373	2014
Leong, C. R. et al. （押海）	A MAVS/TICAM-1-Independent Interferon-Inducing Pathway Contributes to Regulation of Hepatitis B Virus Replication in the Mouse Hydrodynamic Injection Model.	J. Innate Immun.	7	47-58	2015
Kasamatsu, J. et al. （押海）	INAM Plays a Critical Role in IFN-γ Production by NK Cells Interacting with Polyinosinic-Polycytidylic Acid-Stimulated Accessory Cells.	J. Immunol.	193	5199-5207	2014
Takaki, H. et al. （押海）	Dendritic cell subsets involved in type I IFN induction in mouse measles virus infection models.	Int J Biochem Cell Biol.	53C	329-333	2014
Shime, H. et al. （押海）	Myeloid-derived suppressor cells confer tumor-suppressive functions on natural killer cells via polyinosinic:polycytidylic acid treatment in mouse tumor models.	J. Innate Immun.	6	293-305	2014

Okamoto M, et al. （押海）	IPS-1 Is Essential for Type III IFN Production by Hepatocytes and Dendritic Cells in Response to Hepatitis C Virus Infection.	J Immunol.	192(6)	2770-2777	2014
Takaki H. et al. （押海）	MAVS-dependent IRF3/7 bypass of interferon β-induction restricts the response to measles infection in CD150Tg mouse bone marrow-derived dendritic cells.	Mol Immunol.	57(2)	100-110	2014
Tanida I. et al. (鈴木)	Caffeic acid, a coffee-related organic acid, inhibits the propagation of hepatitis C virus.	Jpn J Infect Dis.			In press
Tsukuda S. et al. （鈴木）	Dysregulation of Retinoic Acid Receptor Diminishes Hepatocyte Permissiveness to Hepatitis B Virus Infection through Modulation of NTCP Expression.	J Biol Chem.	I		In press
Matsuda M. et al. （鈴木）	Alternative endocytosis pathway for productive entry of hepatitis C virus.	J Gen Virol.	95	2658-2667	2014
Yamanaka A. et al. （鈴木）	Evaluation of single-round infectious, chimeric dengue type 1 virus as an antigen for dengue functional antibody assays.	Vaccine.	32	4289-4295	2014
Sugiyama N. et al. （鈴木）	Single strain isolation method for cell culture-adapted hepatitis C virus by end-point dilution and infection.	PLoS One.	9	e98168	2014

Ⅳ．　研究成果の刊行物・別刷

Please cite this article in press as: Sato et al., The RNA Sensor RIG-I Dually Functions as an Innate Sensor and Direct Antiviral Factor for Hepatitis B Virus, Immunity (2015), http://dx.doi.org/10.1016/j.immuni.2014.12.016

Immunity
Article

The RNA Sensor RIG-I Dually Functions as an Innate Sensor and Direct Antiviral Factor for Hepatitis B Virus

Seiichi Sato,[1,2,10] Kai Li,[1,2,10] Takeshi Kameyama,[1,2,10] Takaya Hayashi,[3,10] Yuji Ishida,[4] Shuko Murakami,[5] Tsunamasa Watanabe,[5] Sayuki Iijima,[5] Yu Sakurai,[6] Koichi Watashi,[7] Susumu Tsutsumi,[5] Yusuke Sato,[6] Hidetaka Akita,[6] Takaji Wakita,[7] Charles M. Rice,[8] Hideyoshi Harashima,[6] Michinori Kohara,[9] Yasuhito Tanaka,[5] and Akinori Takaoka[1,2,*]

[1]Division of Signaling in Cancer and Immunology, Institute for Genetic Medicine, Hokkaido University, Sapporo, Hokkaido 060-0815, Japan
[2]Molecular Medical Biochemistry Unit, Biological Chemistry and Engineering Course, Graduate School of Chemical Sciences and Engineering, Hokkaido University, Sapporo, Hokkaido 060-0815, Japan
[3]Research Center for Infection-Associated Cancer, Institute for Genetic Medicine, Hokkaido University, Sapporo, Hokkaido 060-0815, Japan
[4]PhoenixBio Co., Ltd., Higashihiroshima, Hiroshima 739-0046, Japan
[5]Department of Virology and Liver Unit, Nagoya City University Graduate School of Medical Sciences, Nagoya, Aichi 467-8601, Japan
[6]Laboratory of Innovative Nanomedicine, Faculty of Pharmaceutical Sciences, Hokkaido University, Sapporo, Hokkaido 060-0812, Japan
[7]Department of Virology II, National Institute of Infectious Diseases, Tokyo 208-0011, Japan
[8]Laboratory of Virology and Infectious Disease, The Rockefeller University, New York, NY 10065, USA
[9]Department of Microbiology and Cell Biology, Tokyo Metropolitan Institute of Medical Science, Setagaya-ku, Tokyo 156-8506, Japan
[10]Co-first author
*Correspondence: takaoka@igm.hokudai.ac.jp
http://dx.doi.org/10.1016/j.immuni.2014.12.016

SUMMARY

Host innate recognition triggers key immune responses for viral elimination. The sensing mechanism of hepatitis B virus (HBV), a DNA virus, and the subsequent downstream signaling events remain to be fully clarified. Here we found that type III but not type I interferons are predominantly induced in human primary hepatocytes in response to HBV infection, through retinoic acid-inducible gene-I (RIG-I)-mediated sensing of the 5′-ε region of HBV pregenomic RNA. In addition, RIG-I could also counteract the interaction of HBV polymerase (P protein) with the 5′-ε region in an RNA-binding dependent manner, which consistently suppressed viral replication. Liposome-mediated delivery and vector-based expression of this ε region-derived RNA in liver abolished the HBV replication in human hepatocyte-chimeric mice. These findings identify an innate-recognition mechanism by which RIG-I dually functions as an HBV sensor activating innate signaling and to counteract viral polymerase in human hepatocytes.

INTRODUCTION

Hepatitis B virus (HBV) is a hepatotropic virus of the *Hepadnaviridae* family and contains a circular, partially double-stranded DNA genome of about 3.2 k base pairs that is replicated via reverse transcription of a pregenomic RNA (pgRNA). HBV causes hepatic inflammation associated with substantial morbidity worldwide (Rehermann and Nascimbeni, 2005; Protzer et al., 2012; Revill and Yuan, 2013). Around four hundred million people worldwide are persistently infected with HBV, which is a major causative factor associated with not only inflammation but also cirrhosis and even cancer of the liver. Currently, interferon (IFN) and nucleoside/nucleotide analogs are available for HBV treatment (Rehermann and Nascimbeni, 2005; Halegoua-De Marzio and Hann, 2014). However, the long-term response rates are still not satisfactory. Elucidation of host immune response against HBV infection is crucial for better understanding of the pathological processes and viral elimination to control HBV infection.

The type I IFNs, IFN-α and IFN-β, are representative cytokines that elicit host innate immune responses against viral infections. In addition, another IFN family, type III IFNs (IFN-λ, also known as IL-28 and IL-29) exhibits potent antiviral activity similar to IFN-α and IFN-β (Sheppard et al., 2003; Kotenko, 2011; Kotenko et al., 2003). Production of type I and type III IFNs is massively induced in many types of cells upon infection with various viruses, which is known to be mediated by the activation of pattern-recognition receptors (PRRs). During virus infection, virus-derived nucleic acids (both RNA and DNA) are mainly sensed by certain PRRs, such as retinoic acid-inducible gene-I (RIG-I) (Yoneyama et al., 2004; Choi et al., 2009; Chiu et al., 2009; Ablasser et al., 2009), melanoma differentiation-associated gene 5 (MDA5) (Yoneyama et al., 2005), cyclic GMP-AMP synthase (cGAS) (Sun et al., 2013), and IFN-γ-inducible protein 16 (IFI16) (Unterholzner et al., 2010). Particularly, RIG-I is a key PRR that can detect virus-derived RNAs in the cytoplasm during infection with a variety of viruses, such as influenza virus, hepatitis C virus (HCV), and measles virus, which are closely related to human disease pathogenesis (Rehwinkel and Reis e Sousa, 2010). Binding of RIG-I to its ligand RNAs, such as 5′-triphosphorylated RNA or short double-stranded RNAs (Takeuchi and Akira, 2009; Hornung et al., 2006), activates the downstream signaling pathways in a manner dependent on the adaptor protein mitochondrial antiviral

signaling protein (MAVS; also known as IPS-1, VISA, or Cardif) (Takeuchi and Akira, 2009), leading to the induction of the IFN-regulatory factor-3 (IRF-3) and NF-κB-dependent gene expression and the subsequent production of type I and type III IFNs and inflammatory cytokines (Takeuchi and Akira, 2009). Thus, RIG-I sensing of viral RNA is a crucial process to activate the antiviral innate responses to limit viral replication and the activation of adaptive immunity (Takeuchi and Akira, 2009).

As for the viruses that are known to be the leading cause of hepatic inflammation, RIG-I is the major PRR that initiates innate immune responses against HCV. RIG-I sensing of HCV is mediated through its recognition of the poly-U/UC motif of the HCV RNA genome 3′ nontranslated region, which leads to the activation of type I IFN response (Saito et al., 2008). On the other hand, earlier studies have shown that the innate immune activation is impaired and the induction of type I IFNs such as IFN-α or IFN-β is hardly detected in animal models of HBV infection, as compared with HCV infection (Wieland et al., 2004; Nakagawa et al., 2013). However, it is still not fully clarified how HBV is recognized by human hepatocytes and the role of type III IFNs as well.

Here we report that HBV infection predominately induces type III, but not type I, IFN gene induction, which is mediated by RIG-I through its recognition of the 5′-ε region of HBV-derived pgRNA. We also show that RIG-I can counteract the interaction of HBV polymerase (P protein) with the 5′-ε region of pgRNA in an RNA-binding dependent manner, resulting in the suppression of HBV replication. Furthermore, liposome-mediated delivery and expression of the 5′-ε region-derived RNA in liver suppressed the HBV replication in vivo in chimeric mice with humanized livers. Thus, our findings demonstrate the innate defense mechanisms based on the viral RNA-RIG-I interaction, whereby RIG-I functions not only as a HBV sensor for the activation of IFN response but also as a direct antiviral factor.

RESULTS

Type III IFNs Are Predominantly Induced in Hepatocytes during HBV Infection

To investigate the innate immune activation during HBV infection, we examined type I and type III IFN responses in human hepatocytes. Consistent with the previous reports (Wieland et al., 2004; Nakagawa et al., 2013), we hardly observed the induction of type I IFNs, IFN-α4, and IFN-β in response to transfection with plasmids carrying 1.24-fold the HBV genome of three major different genotypes, Ae (HBV-Ae), Bj (HBV-Bj), and C (HBV-C) (Figure 1A and Figure S1A available online) at least up to seven days after transfection, although the expression of HBV RNAs was detectable (Figure S1B). On the other hand, type III IFN, IFN-λ1, was induced in all of the three types of human hepatocyte cell line tested (Figures 1A and S1A). In HepG2 cells, HBV-C shows the highest IFN-λ1 response, which was also confirmed by ELISA, albeit weakly (Figures 1A and 1B). Moreover, IFN-λ1 in culture supernatant could inhibit vesicular stomatitis virus (VSV) replication in plaque reduction assay, as well as HBV replication (Figure S1C), indicating the physiological relevance of the induced IFN-λ1 to antiviral activities. Consistent with these results, we observed the significant induction of not only IFN-λ1 but also IFN-λ2 and -λ3 in primary human hepatocytes (PHH) in vitro 24 hr after infection with HBV-C (Figure 1C); however, neither of type I nor type II IFN tested was induced (Figures S1D and S1E). Although it is difficult to simply compare the amount of IFN induced by different types of virus, the induction of IFN-λ1, λ2, and λ3 mRNAs in response to HBV infection was much weaker than that of Newcastle disease virus (NDV) infection (Figure 1C). In this regard, in order to rule out the possibility that the IFN-λ response is due to contaminants in the inocula, we used Lamivudine (LAM), an HBV inhibitor, in this assay. Treatment with LAM inhibited IFN-λ mRNA induction in response to HBV infection in PHH (Figure 1C), suggesting that the IFN response is actually induced by HBV replication. Furthermore, we analyzed HepG2-sodium taurocholate cotransporting polypeptide (NTCP)-C4 cell line (Iwamoto et al., 2014) stably expressing human NTCP, a functional receptor for HBV (Yan et al., 2012), and confirmed that IFN-λ1 and IFN-inducible genes such as *OAS2* and *RSAD2*, but not IFN-β, were induced in these cells after infection with HBV-C, and that these inductions were abolished by treatment with LAM (Figure 1D). To next assess the innate immune responses in vivo during HBV infection, we exploited severe combined immunodeficiency mice that carry the urokinase-type plasminogen activator transgene controlled by an albumin promoter ($uPA^{+/+}$/SCID mice), in which more than 70% of murine hepatocytes were replaced by human hepatocytes (Tateno et al., 2004) (hereinafter referred to as chimeric mice). After the chimeric mice were intravenously infected with HBV-C, which was derived from patients with chronic hepatitis, the expression of type III IFN mRNAs increased in the liver tissue, whereas IFN-α4 and IFN-β mRNAs were not upregulated (Figure 1E). In parallel with this type III IFN response, we also observed the expression of IFN-inducible genes, such as *CXCL10*, *OAS2*, and *RSAD2*, in the human liver of these infected mice (Figure 1E). These findings indicate that a moderate type III but not type I or type II IFN response is activated in human hepatocytes in response to HBV infection.

HBV-Induced Type III IFN Expression Depends on RIG-I

We next determined which sensor-mediated signaling pathway is responsible for the HBV-induced type III IFN response. As HBV is a DNA virus (Rehermann and Nascimbeni, 2005; Protzer et al., 2012; Revill and Yuan, 2013), we assessed the contribution of previously reported cytosolic DNA sensors including RIG-I (Chiu et al., 2009; Ablasser et al., 2009; Choi et al., 2009), IFI16 (Unterholzner et al., 2010), and cGAS (Sun et al., 2013) in human hepatocytes. Knockdown analyses revealed that IFN-λ1 induction in HepG2 or Huh-7 cells by plasmid transfection for HBV-C or HBV-Ae, respectively, was suppressed by the knockdown of RIG-I, but not that of the other sensors (Figures 2A, S2A and S2B). To further confirm the involvement of RIG-I in HBV-triggered type III IFN response, we measured IFN-λ1 mRNA expression induced by plasmid expression in Huh-7.5 cells that carry a dominant-negative mutant RIG-I allele that prevents RIG-I signaling (Saito et al., 2007), as compared with Huh-7 cells that have an intact RIG-I pathway. Huh-7.5 cells failed to induce IFN-λ1 mRNA expression in response to HBV-Ae genome plasmid transfection, as in the case of stimulation with 5′-triphosphate RNA (3pRNA), a RIG-I ligand (Takeuchi and Akira, 2009; Hornung et al., 2006) (Figure 2B). In concordance with this result, knockdown of tripartite motif containing protein

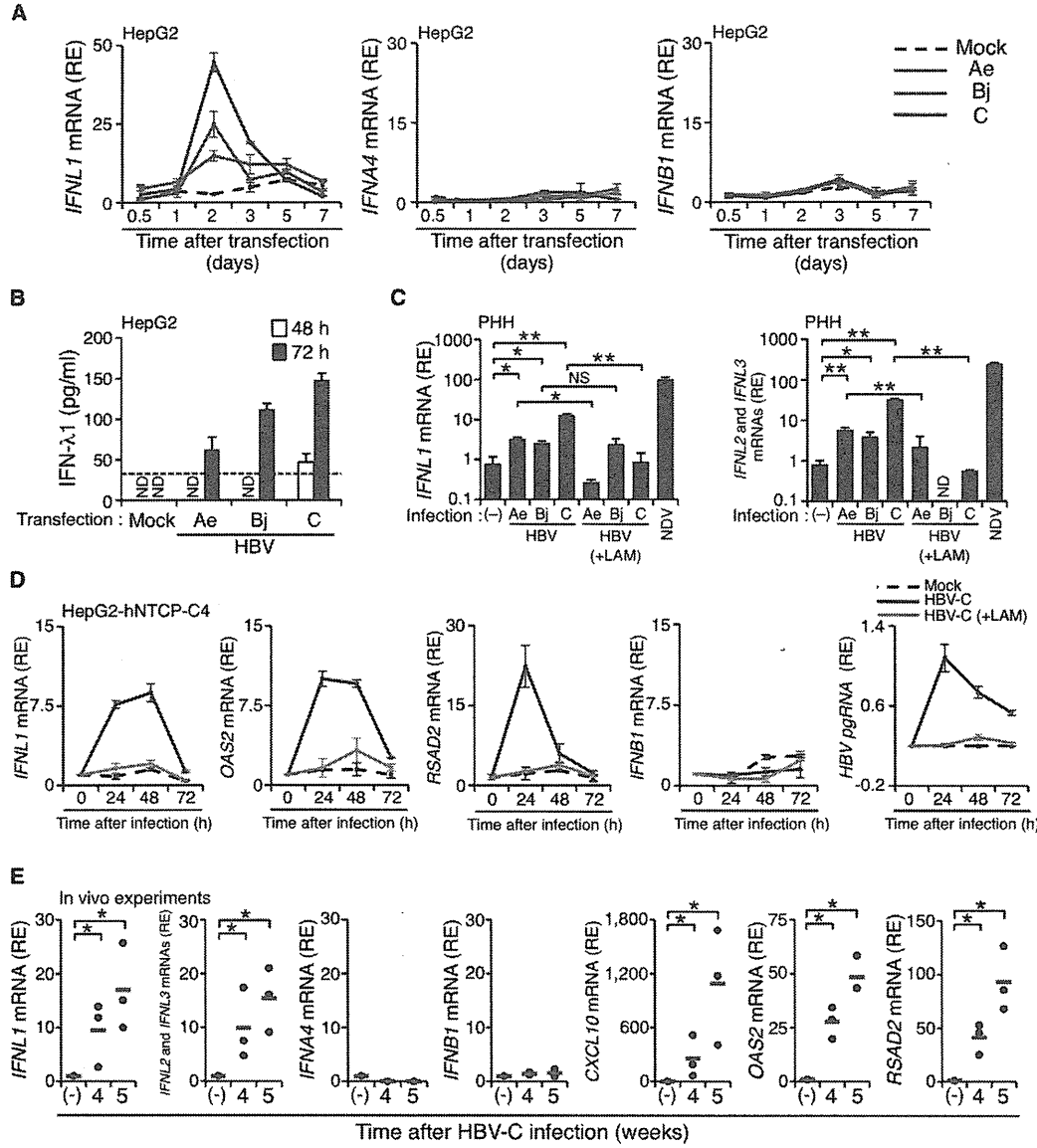

Figure 1. IFN-λ Induction in Human Hepatocytes in Response to HBV Infection

(A) Quantitative RT-PCR (qRT-PCR) analysis of *IFNL1* (left), *IFNA4* (middle), and *IFNB1* (right) mRNA at the indicated times after transfection with 1.24-fold the HBV genome (genotype Ae, Bj, or C) or empty vector (Mock) in HepG2 cells.

(B) ELISA of IFN-λ1 at 48 or 72 hr after transfection with the HBV genome in HepG2 cells. The dot line indicates the minimum detectable amount (31.2 pg/ml) of IFN-λ1 by the ELISA kit. ND, not detected, indicates below the minimum detectable amount.

(C) qRT-PCR analysis of *IFNL1*, *IFNL2*, and *IFNL3* mRNA at 24 hr after infection with HBV, NDV (multiplicity of infection = 10) or mock (–), or media-treated Lamivudine (LAM) as control in primary human hepatocytes (PHH). The mRNA copy number (±SD) of each subtype of type III IFN per 1 μg total RNA upon HBV-C infection is as follows: *IFNL1* (83,197.6 ± 6,241.4) and *IFNL2/3* (409,280.6 ± 119,676.2).

(D) Time course analyses by qRT-PCR of *IFNL1*, *OAS2*, *RSAD2*, *IFNB1* mRNA, and *pgRNA* at the indicated times after HBV infection in HepG2-hNTCP-C4 cells. The effect of Lamivudine treatment was also analyzed.

(E) qRT-PCR analysis of *IFNL1*, *IFNL2*, *IFNL3*, *IFNA4*, *IFNB1*, *CXCL10*, *OAS2*, and *RSAD2* mRNA of liver tissues at 4 or 5 weeks after infection with HBV-C in chimeric mice. (–), uninfected mice. Red lines represent the mean of each dataset. *$p < 0.05$ and **$p < 0.01$ versus control. RE, relative expression. (A–D) Data are presented as mean and SD (n = 3) and are representative of at least three independent experiments. See also Figure S1.

25 (TRIM25), MAVS, TANK-binding kinase 1 (TBK1), and IRF-3, all of which are signaling molecules essentially involved in the RIG-I-mediated IFN pathway (Takeuchi and Akira, 2009), resulted in the suppression of IFN-λ1 mRNA induction in HepG2 cells in response to transfection with the HBV-C genome. On the other hand, such an effect was not observed in cells treated

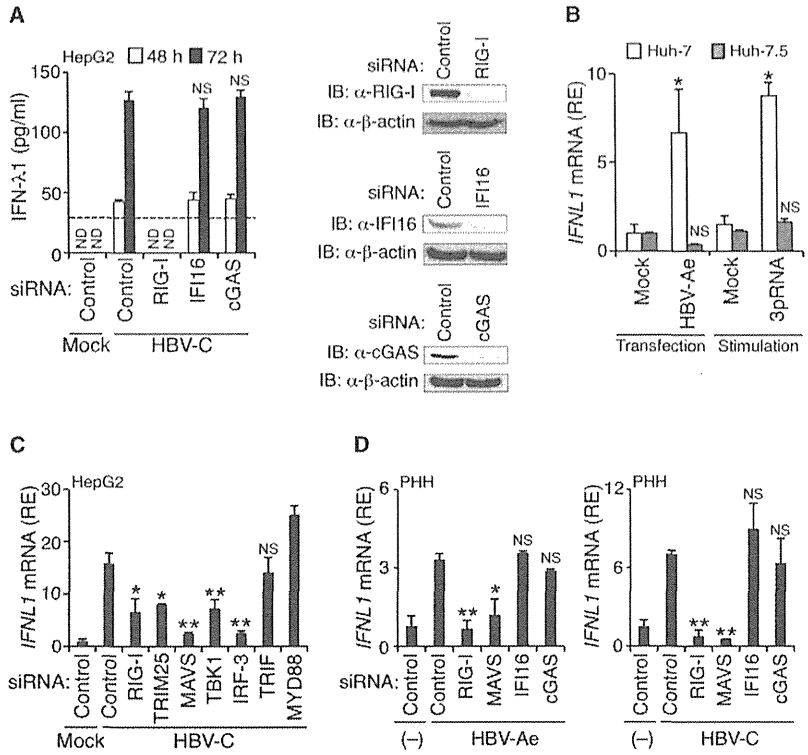

Figure 2. RIG-I-Dependent IFN-λ Induction in Response to HBV Infection

(A) HepG2 cells treated with control siRNA (Control) or siRNA targeting RIG-I, IFI16, or cGAS were transfected with the HBV-C genome for 48 or 72 hr. The amount of IFN-λ1 were measured by ELISA. The dot line indicates the minimum cytokine expression detected (31.2 pg/ml) of IFN-λ1 by the ELISA kit. ND, not detected, indicates below detectable concentrations (left), and knockdown efficiency was analyzed by immunoblotting (IB) (right).

(B) qRT-PCR analysis of *IFNL1* mRNA in Huh-7 or Huh-7.5 cells transfected with the HBV-Ae genome (at 24 hr after transfection) or stimulated with 3pRNA (1 μg/ml) for 6 hr.

(C) HepG2 cells treated with control siRNA (Control) or the indicated siRNAs were transfected with the HBV-C genome. At 48 hr after transfection, total RNAs were subjected to qRT-PCR analysis for *IFNL1*.

(D) qRT-PCR analysis of *IFNL1* mRNA in siRNA-treated PHH at 24 hr postinfection with indicated HBV genotype. Mock, empty vector-transfected. (–), uninfected. Data were normalized to the expression of *GAPDH*. Data are presented as mean and SD (n = 3) and are representative of at least three independent experiments. *$p < 0.05$ and **$p < 0.01$ versus control in (B) or HBV-infected control group in (A, C, and D). NS, not significant. See also Figure S2.

with either TRIF (also known as TICAM-1) or MYD88 siRNA (Figures 2C and S2C). In addition, we confirmed that the knockdown of RIG-I and MAVS abolished IFN-λ1 induction in PHH infected with each genotype (Figure 2D). Furthermore, we also confirmed by knockdown assay that the induction of IFN-λ1 and OAS2 mRNA in HepG2-hNTCP-C4 cells in response to infection with HBV-C was dependent on RIG-I (Figure S2E). These data indicate that IFN-λ1 gene induction during HBV infection depends largely on RIG-I signaling pathway.

The 5′-ε Region of HBV pgRNA Is a Key Element for RIG-I-Dependent IFN-λ1 Induction

RIG-I can recognize not only virus-derived RNA but also DNA in the cytoplasm (Yoneyama et al., 2004; Choi et al., 2009; Chiu et al., 2009; Ablasser et al., 2009). To further clarify how RIG-I recognizes HBV, we first examined either or both of which nucleic acid (DNA and RNA) derived from HBV-infected cells can activate IFN-λ1 gene expression. Transfection with nucleic acid fractions extracted from HBV infected Huh-7 cells after pretreatment with RNase A, but not DNase I resulted in marked inhibition of the *IFNL1* promoter activation, suggesting that virus-derived RNAs might be candidates of the RIG-I ligand during HBV infection (Figure 3A).

The HBV genome comprises a partially double-stranded 3.2 kb DNA. During a life cycle of HBV in hepatocytes, its covalently closed circular DNA (cccDNA) is transcribed to generate four major RNA species: the 3.5, 2.4, 2.1, and 0.7 kb viral RNA transcripts (Rehermann and Nascimbeni, 2005; Protzer et al., 2012; Revill and Yuan, 2013). We created an siRNA to suppress the expression of all of these RNA transcripts and tested its effect on HBV-induced IFN-λ1 expression. As shown in Figure 3B, knockdown with this siRNA (Figure S3A) suppressed IFN-λ1 induction in Huh-7 cells transfected with HBV-Ae. Next, to determine which of these HBV RNA transcripts is/are involved in the RIG-I-mediated IFN-λ1 induction, we prepared expression vectors to express each of these four viral transcripts in HEK293T cells that are often used to analyze RIG-I signaling pathway in human cells. As a result, it is only the longest 3.5 kb transcript, that is, pgRNA, that has the potential to elicit a significant induction of IFN-λ1 mRNA (Figures 3C and S3B). It was also confirmed by knockdown analysis with pgRNA-targeted siRNA, which showed significant suppression of IFN-λ1 induction in HepG2 cells transfected with HBV-Ae (Figure S3C). These results suggest that 5′-1.1 kb region of HBV pgRNA is critical for the activation of RIG-I pathway to induce IFN-λ1 expression. On the other hand, the remaining three transcripts, which also contain the same sequence of part of this 1.1 kb region of HBV pgRNA at the 3′ end of their transcripts, failed to induce IFN-λ1 mRNA (Figure 3C). An artificially deleted form of pgRNA, which lacks this overlapping sequence at the 3′-region (Δ3), showed IFN-λ1 induction, whereas such response was not observed for another mutant pgRNA lacking it at the 5′-region (Δ5) (Figure 3D). These data also support a possible important role of the 5′-overlapping sequence of HBV pgRNA for RIG-I-mediated IFN-λ1 induction.

The 5′-end of HBV pgRNA is known to contain the encapsidation sequence, called "epsilon (ε)," which takes a stem-loop secondary structure (Junker-Niepmann et al., 1990; Pollack and

Please cite this article in press as: Sato et al., The RNA Sensor RIG-I Dually Functions as an Innate Sensor and Direct Antiviral Factor for Hepatitis B Virus, Immunity (2015), http://dx.doi.org/10.1016/j.immuni.2014.12.016

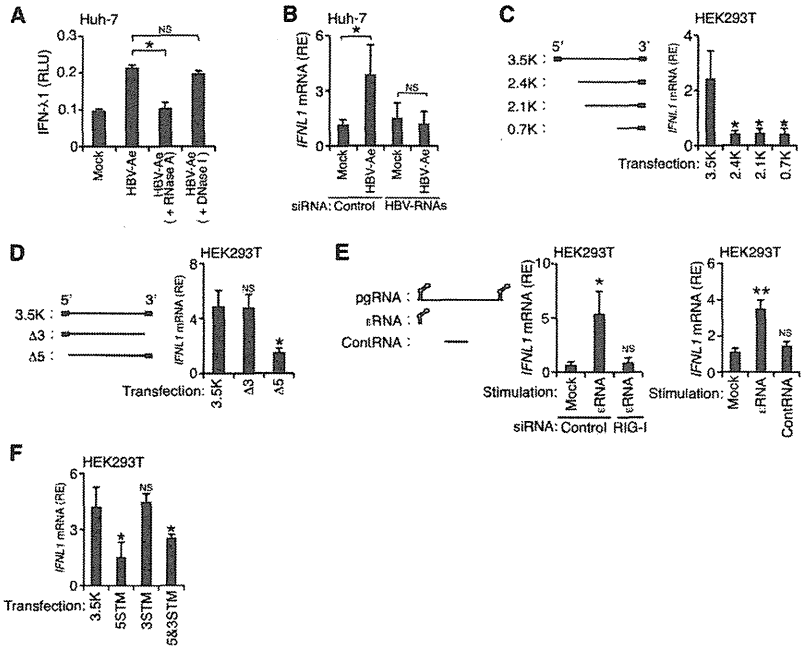

Figure 3. RIG-I Activation Is Mediated by Its Recognition of the 5′-ε Region of HBV pgRNA

(A) Luciferase activity of an IFN-λ1 reporter plasmid after 24 hr of stimulation with nucleic acids (2 μg/ml) extracted from Huh-7 cells transfected with control plasmid (Mock) or the HBV-Ae genome with or without RNase A or DNase I treatment. RLU, relative luciferase units.

(B) Huh-7 cells treated with control or HBV RNA-targeted siRNA were transfected with the HBV-Ae genome or mock. After 24 hr of transfection, total RNAs were subjected to qRT-PCR for *IFNL1*.

(C and D) A schematic representation of four types of HBV RNAs, pgRNA (3.5 kb), 2.4 kb, 2.1 kb, and 0.7 kb RNAs in (C), and two deleted forms of pgRNA, Δ5 and Δ3, in (D). The overlapping region is shown in blue. qRT-PCR analysis of *IFNL1* mRNA of HEK293T cells after 24 hr of transfection with the indicated expression vectors. Data were normalized to the amount of each HBV RNA expression (C and D).

(E) A schematic representation of pgRNA, εRNA, or control RNA (ContRNA) (left). HEK293T cells treated with control or RIG-I siRNA were unstimulated (Mock) or stimulated with εRNA for 12 hr. Total RNAs were subjected to qRT-PCR for *IFNL1* (middle). qRT-PCR analysis of *IFNL1* mRNA in HEK293T cells after 12 hr of stimulation with εRNA or ContRNA (right). Each of the RNAs was prepared by in vitro transcription.

(F) HEK293T cells were transfected with each plasmid for stem-loop mutants of pgRNA (5STM, 3STM, or 5 and 3STM), and then subjected to qRT-PCR analysis as described in (C). *$p < 0.05$ and **$p < 0.01$ versus control in (A, B, and E) or versus 3.5K in (C, D, and F). NS, not significant. See also Figure S3.

Ganem, 1993; Knaus and Nassal, 1993; Jeong et al., 2000). Therefore, we hypothesized that this 5′-ε structure might confer a possible pathogen-associated molecular pattern (PAMP) motif for RIG-I recognition. To test this hypothesis, we stimulated HEK293T and HepG2 cells with the ε region-derived RNA (hereafter called εRNA). Consequently, IFN-λ1 mRNA was significantly induced, which was dependent on RIG-I, while such a response was not detected upon stimulation with the equivalent length of RNA that is derived from HBV pgRNA but does not contain any ε element (ContRNA) (Figure 3E and S3D). We also confirmed RIG-I-dependent IRF-3 activation in response to stimulation with εRNA (Figures S3D and S3E). Due to the overlapping sequence of 5′- and 3′-ends of HBV pgRNA as mentioned above, this ε element is found at both ends of pgRNA. We next generated several mutant forms of HBV pgRNA, each of which carries mutations within 5′- or 3′-ε region or both to disrupt the stem-loop structure (5STM, 3STM, or 5 and 3STM, respectively). In concordance with the results shown in Figures 3C and 3D and S3B, IFN-λ1 mRNA induction was detected upon expression of the 3STM transcript that has an intact 5′-ε region, as similar to that of intact 3.5-kb pgRNA (Figure 3F). In contrast, either 5STM or 5 and 3STM did not show significant response. These findings indicate that the 5′-ε region of HBV pgRNA is critical for IFN-λ1 induction possibly through the recognition by RIG-I.

RIG-I Interacts with the ε-Region of pgRNA

Next, we assessed the interaction of RIG-I with the ε region of HBV pgRNA, that is, εRNA. Pull-down assays showed that Flag-tagged RIG-I was coprecipitated with εRNA, but not with ContRNA, in HEK293T cells (Figure 4A, top). Similarly, endogenous RIG-I interacted with εRNA albeit weakly (Figure 4A, bottom). We also demonstrated the intracellular colocalization of RIG-I with εRNA in Huh-7.5 cells (Figure 4B). In addition, RNA-binding protein immunoprecipitation (RIP) assay revealed that the full length of HBV pgRNA was detected in the RIG-I-immunoprecipitated complex, and Δ5 pgRNA and Δ3 pgRNA were also detected (Figure S4A), which is seemingly inconsistent with the results by the functional assay (Figures 3C, 3D, 3F and S3C). These results suggest that the ε region is required for its interaction with RIG-I, but only the 5′-ε region is necessary to activate RIG-I pathway. We further tried to determine which region of RIG-I mediates its interaction with HBV pgRNA. Both RIP assay and RNA pull-down assay with several deletion mutants of RIG-I showed that the C-terminal portion of RIG-I (C-RIG) including its helicase domain and repressor domain (RD) except for CARDs can bind to HBV pgRNA (Figure 4C; Figures S4B and S4C). In addition, gel shift assay showed that the interaction of HBV εRNA or pgRNA was impaired with the RD or C-RIG mutant, respectively, each of which carries a point mutation (K888E) that abolishes its RNA-binding activity (Cui et al., 2008) (Figure 4D). A similar result was also obtained by RIP assay, wherein the wild-type (WT) C-RIG, but not the K888E mutant, was coimmunoprecipitated with HBV pgRNA (Figure S4D), like HCV RNA that was previously reported to interact with RIG-I (Figure S4E). We also confirmed the interaction of HBV pgRNA with endogenous RIG-I in HepG2 cells, whereas its interaction with other nucleic acid sensors, such as IFI16 and MDA5 (Yoneyama et al., 2005), was not detected (Figure 4E). These data indicate that

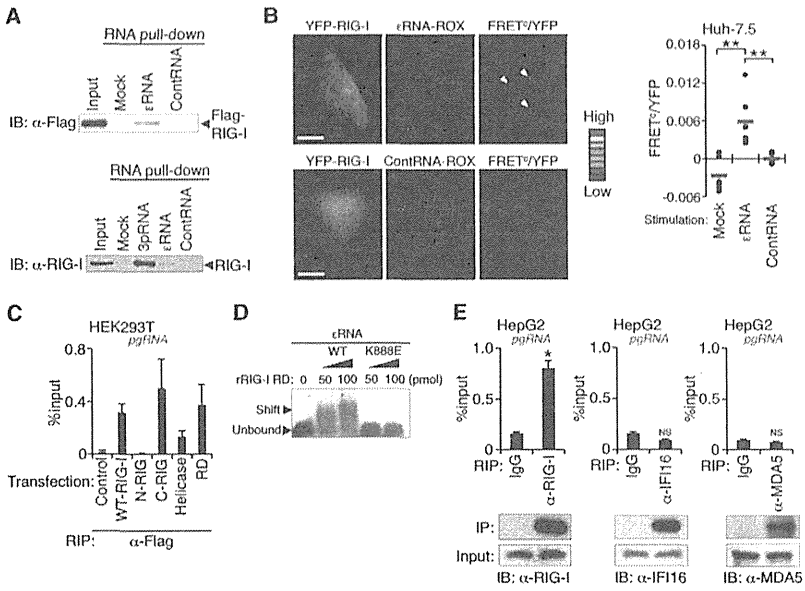

Figure 4. RIG-I Interacts with the ε Region of pgRNA

(A) RNA pull-down assay showing the binding activity of the indicated RNAs to Flag-tagged RIG-I (Flag-RIG-I) in HEK293T cells (top) or endogenous RIG-I in HepG2 cells (bottom).

(B) FRET analysis for the interaction of YFP-tagged RIG-I (YFP-RIG-I) with rhodamine (ROX)-conjugated εRNA (εRNA-ROX) or ContRNA (ContRNA-ROX). Representative fluorescence images of YFP, ROX, and $FRET^C$/YFP (the ratio of corrected FRET ($FRET^C$) to YFP). Arrowheads indicate area showing high FRET efficiency. Scale bar represents 20 μm. Right, dot plot of $FRET^C$/YFP ratio (small horizontal bars, mean).

(C) RIP assay with HEK293T cell lysates expressing several Flag-tagged deletion mutants of RIG-I and pgRNA expression vector by using anti-Flag antibody. Immunoprecipitated pgRNA was quantitated by qRT-PCR and normalized to the amount of immunoprecipated proteins (Figure S4C) and is represented as fraction of input RNA prior to immunoprecipitation (percentage input).

(D) Gel-shift analysis of complex formation between εRNA and recombinant RIG-I RD (WT) or RD (K888E). Arrowheads denote position of unbound RNA and RNA–RIG-I complexes.

(E) RIP assay with HepG2 cell lysates prepared after 48 hr of transfection of the HBV-C genome by using anti-RIG-I, anti-IFI16, anti-MDA5, or control immunoglobulin G. The immunoprecipitated pgRNA was measured by qRT-PCR (top) as described in (C). Whole-cell expression and immunoprecipitated amounts of RIG-I, IFI16, and MDA5 (bottom). Data are presented as mean and SD (n = 3) and are representative of at least three independent experiments. *$p < 0.05$ and **$p < 0.01$ versus control in (B and E). NS, not significant. See also Figure S4.

the 5′-ε region of viral pgRNA functions as an HBV-associated molecular pattern to be specifically recognized by RIG-I and can trigger IFN-λ response.

RIG-I Exerts an Antiviral Activity by Counteracting the Interaction of HBV Polymerase with pgRNA

We next assessed the contribution of RIG-I pathway in antiviral defense against HBV infection. RIG-I knockdown in PHH resulted in a higher HBV genome copy number at 10 days after infection with HBV-C, as compared with PHH treated with control siRNA (Figure 5A). A similar observation was made for RIG-I siRNA-treated HuS-E/2 cells (Figure S5A). These results indicate an implicated role of RIG-I as an innate sensor to activate antiviral response against HBV infection. On the other hand, it has been previously reported that the 5′-ε region of HBV pgRNA is important to serve as a binding site of viral P protein for initiating reverse transcription (Bartenschlager and Schaller, 1992). As consistent with this, we showed that the P protein interacts with εRNA in Huh-7.5 and HEK293T cells, by fluorescence resonance energy transfer (FRET) analysis (Figure 5B) and RNA pull-down assay (Figure S5B), respectively. These findings facilitated us to examine whether RIG-I could block the access of P protein toward the ε region. As we expected, recombinant RIG-I protein suppressed the interaction of P protein with pgRNA in a dose-dependent manner (Figure 5C). Such an inhibitory effect was also observed in Huh-7.5 cells by expression of WT RIG-I, as well as its T55I (Sumpter et al., 2005; Saito et al., 2007) or K270A (Takahasi et al., 2008) mutant (Figures 5D and S5C), both of which are not able to induce ligand-dependent activation of the downstream signaling but retain their RNA-binding activities. On the other hand, the K888E (Cui et al., 2008) mutant could not inhibit the binding of P protein with pgRNA (Figures 5D and S5C). In addition, treatment with recombinant IFN-λ1 in Huh-7.5 cells upregulated the amount of the mutant RIG-I protein (T55I) (Figure S5D), resulting in a partial inhibition of the P protein interaction with pgRNA, and this inhibitory effect was abrogated by RIG-I knockdown (Figure 5E). In fact, FRET analysis showed that the P protein-εRNA interaction was significantly suppressed by expression of the RIG-I RD (WT) alone, but not the mutant RD (K888E) (Figure S5E). Furthermore, HBV replication was also suppressed by expression of the RIG-I RD (WT) in Huh-7.5 cells, wherein any IFN induction is not observed, while the mutant RD (K888E) did not affect viral replication (Figure 5F). These findings revealed another aspect of RIG-I as a direct antiviral factor through its interference with the binding of HBV P protein to pgRNA in an IFN pathway-independent manner.

The εRNA Restricts HBV Replication in Human Hepatocyte-Chimeric Mice

Lastly, based on the above results, we tried to harness the therapeutic potential of the P protein-interacting εRNA for the control of HBV infection. A vector was designed to include a 63 bp DNA oligo, which is transcribed into an εRNA. We confirmed in the in vitro experiments using Huh-7.5 cells that εRNA induced by this vector-driven expression is capable to function as a decoy RNA to interfere with the binding of HBV P protein to pgRNA and to inhibit viral replication in an IFN-independent manner (Figures 6A and 6B, left). On the other hand, εRNA did not show any difference in HCV replication as compared with control (Figure 6B, right). In order to evaluate the therapeutic efficacy of εRNA in vivo, we exploited HBV infection model of human

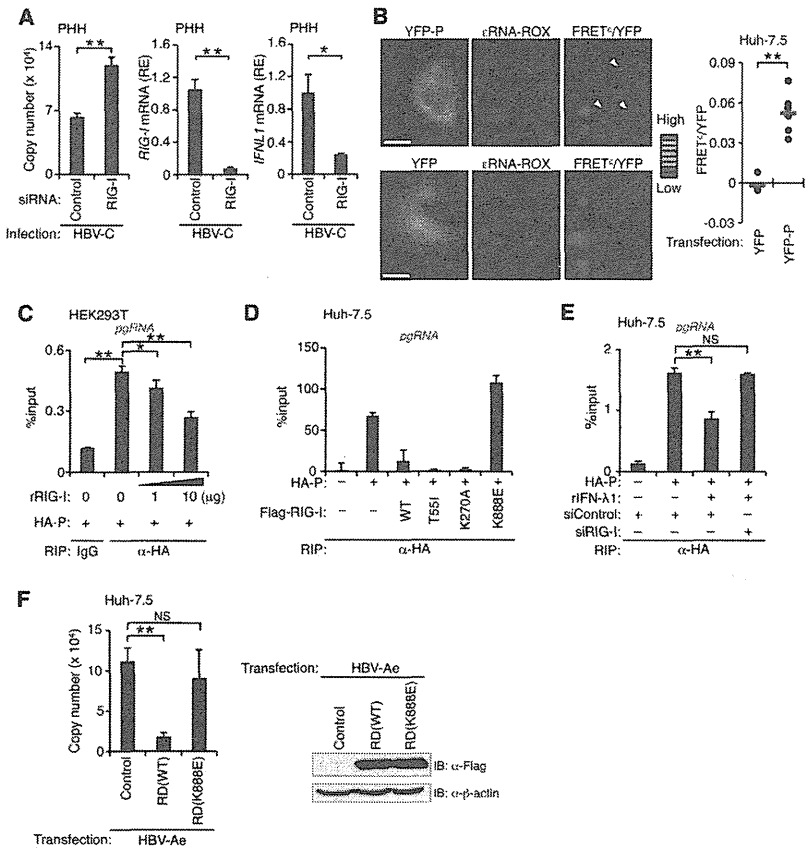

Figure 5. RIG-I Functions as an Antiviral Factor by Counteracting the Interaction of HBV P Protein with pgRNA

(A) qPCR analysis of copy numbers of encapsidated HBV DNA (left) and qRT-PCR analysis of *RIG-I* (middle) and *IFNL1* mRNA (right) in control or RIG-I siRNA-treated PHH after 10 days of infection with HBV-C.

(B) FRET analysis for the interaction between YFP-tagged P protein (YFP-P) or YFP and εRNA-ROX as described in Figure 4B. Scale bar represents 20 μm. Arrowheads indicate area showing high FRET efficiency.

(C) HEK293T cell lysates expressing pgRNA and HA-tagged P protein (HA-P) were incubated with the indicated amount of recombinant RIG-I (rRIG-I). The interaction of pgRNA with HA-P was analyzed by RIP assay and qRT-PCR analysis as described in Figure 4C.

(D) Cell lysates from Huh-7.5 cells expressing HBV pgRNA, HA-P, and Flag-RIG-I or its mutants as indicated were subjected to RIP assay for the characterization of the capability of RIG-I to counteract the interaction of pgRNA with HA-P, as described in Figure 4C.

(E) The effect of rIFN-λ1 treatment on the interaction of pgRNA with HA-P in Huh-7.5 cells was assessed by RIP assay. Huh-7.5 cells expressing both pgRNA and HA-P were treated with rIFN-λ1 (100 ng/ml) for 24 hr, and subjected to RIP assay as described in Figure 4C. RIG-I dependency was also determined by RIG-I knockdown analysis.

(F) Huh-7.5 cells were transfected with an expression vector for RIG-I RD (WT) or RD (K888E), together with the HBV-Ae genome. After 72 hr of transfection, copy numbers of encapsidated HBV DNA were measured (left), as described in (A). Expression of Flag-RIG-I RD (WT) and RD (K888E) (right). *$p < 0.05$ and **$p < 0.01$ versus control. NS, not significant. See also Figure S5.

hepatocyte-chimeric mice. HBV-infected mice underwent intravenous administration with the εRNA expression vector loaded in a liposomal carrier, a multifunctional envelope-type nanodevice (MEND) for efficient delivery, for 2 weeks. Treatment with εRNA-MEND significantly suppressed the elevation of the number of viral genome copies in the sera by less than one tenth of those for control mice (Figure 6C). Consistently, immunofluorescence analyses showed that the expression of HBV core antigen (HBcAg) in the liver tissues of εRNA-MEND-treated chimeric mice was remarkably reduced as compared with those of control mice (Figure 6D).

DISCUSSION

The innate immune system acts as a front line of host defense against viral infection. In this step, PRRs play a crucial role in the recognition of invading viruses. In particular, nucleic acid sensing of viruses is central to the initiation of antiviral immune responses. In this study, we tried to seek for a relevant nucleic acid sensor(s) for HBV and to characterize the IFN response during HBV infection. As a result, we have identified RIG-I as an important innate sensor of HBV to predominantly induce type III IFNs in hepatocytes through its recognition of the 5′-ε stem-loop of HBV pgRNA (Figures 1, 2, 3, and 4). In this respect, there have also been several reports showing that HBV X or P protein interacts with MAVS or competes for DDX3 binding with TBK1, respectively (Wei et al., 2010; Wang and Ryu, 2010; Yu et al., 2010), and inhibits RIG-I-mediated type I IFN pathway, which possibly enables HBV to evade from antiviral innate immune response. This would mirror the important role of RIG-I-mediated signaling for antiviral defense against HBV infection, although further investigation will be required to determine whether other sensing molecules except for RIG-I are engaged in the activation of innate responses in other cell types including dendritic cell subsets. Interestingly, Lu et al. have recently showed that the genotype D of HBV is sensed by MDA5, but not RIG-I, which is based only upon the analyses with HBV genome (2-fold) plasmid transfection in a single cell line Huh-7 (Lu and Liao, 2013). In this respect, we presume that such seemingly contradictory results might arise mainly from the difference in HBV genotype: It has been reported that the genotype D is phylogenetically different from the genotypes A, B, and C, which we analyzed in this study (Kato et al., 2002).

In addition, according to our results (Figure 1C and S1C), HBV-induced type III IFN response does not seem to be efficient as compared with the case with NDV infection. We speculate that

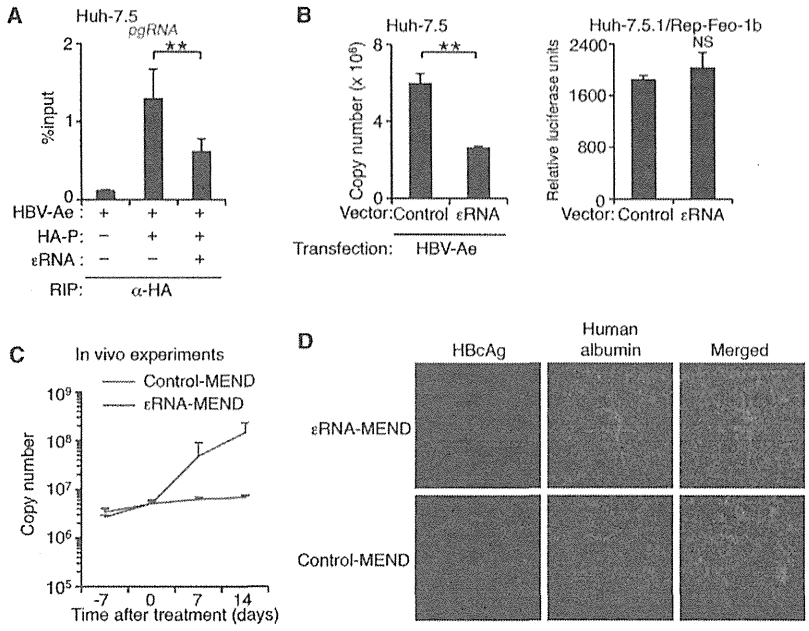

Figure 6. Inhibition of HBV Replication by εRNA

(A) Huh-7.5 cells were transfected with expression vectors for HA-P and εRNA, together with the HBV-Ae genome. RIP assay was performed to evaluate the effect of εRNA on the interaction between HA-P and pgRNA, as described in Figure 5D.

(B) Copy numbers of encapsidated HBV DNA in Huh-7.5 cells expressing the HBV-Ae genome and εRNA, as determined by qPCR (left). HCV replication in Huh-7.5.1/Rep-Feo-1b cells expressing εRNA, as determined by luciferase assay (right).

(C) HBV-infected mice were intravenously administrated with the εRNA expression vector (εRNA-MEND) or empty vector (Control-MEND) loaded in liposomal carrier at a dose of 0.5 mg/kg of body weight every 2 days for 14 days. Serum HBV DNA in HBV-infected chimeric mice was determined by qPCR (n = 3 per group). Day 0 indicates the time of the initiation of administration.

(D) Immunofluorescence imaging was performed for the detection of HBcAg (red) and human albumin (green) in the liver sections of HBV-infected chimeric mice at 14 days after treatment with εRNA-MEND or Control-MEND as described in Experimental Procedures. Data are presented as mean and SD (n = 3) and are representative of at least three independent experiments. $^{**}p < 0.01$ versus control. NS, not significant.

the weakness of the IFN response during HBV infection might attribute at least in part to these viral evasions from host-cell control, which would be supported by our preliminary data showing that one HBV mutant, which generates viral RNAs including pgRNA but lacks the ability to express whole viral proteins including HBV X and P proteins, can induce higher amounts of IFN-λ1 than intact HBV (Figure S1G). In relevance with this, our present data indicate that the interaction of HBV P protein with the 5′-ε stem-loop affects the RIG-I-mediated recognition of viral pgRNA and the subsequent downstream signaling events, which might likely suppress the induction of IFN-λs. This might provide an aspect of HBV P protein in terms of viral evasion from RIG-I activation. As for the mechanism for the preferential induction of type III IFNs in hepatocytes in response to HBV, as well as HCV (Nakagawa et al., 2013; Park et al., 2012), we might speculate the existence of a hepatocyte-specific factor(s), which is selectively involved in type III IFN gene induction, although this issue merits further investigation including epigenetic evaluation of human hepatocytes. We also found that either of the 5′- or 3′-ε region of pgRNA could interact with RIG-I but it was only the 5′-ε region that contributed to the induction of IFN-λ1 (Figures 3D and S4A). In this respect, we presume that some cofactor(s) might additionally determine the preferential use of the 5′-ε region for RIG-I activation; however, it would be a next interesting issue to be solved. In addition to this, our data demonstrated a hitherto-unidentified function of RIG-I as a direct antiviral factor against HBV infection (Figure 5). Mechanistically, RIG-I was found to counteract the accessibility of HBV P protein to the 5′-ε stem-loop of pgRNA, which is an important process for the initiation of viral replication (Bartenschlager and Schaller, 1992). As is the case with this, several viral PAMPs known to be recognized by RIG-I, for example, the poly-U/UC tract in the 3′ nontranslated region of HCV genome (Saito et al., 2008) and 5′ terminal region of influenza virus genome (Baum et al., 2010) were previously reported to be directly or indirectly critical for viral replication (You and Rice, 2008; Huang et al., 2005; Moeller et al., 2012). In this respect, one could envisage that such an exquisite targeting by RIG-I would confer a unique machinery to ensure efficient antiviral activities of RIG-I. Therefore, RIG-I is likely to play dual roles as an innate sensor and as a direct antiviral effector for host defense during viral infection.

In relation to the evaluation of the experiments shown in Figures 6C and 6D, we additionally analyzed the following points: When we treated HepG2 cells with εRNA-MEND or Control-MEND, in both cases we hardly detected the massive induction of cytokines such as *TNF*, *IL6*, and *CXCL10* (data not shown). This was further confirmed by analyzing SCID mice injected with εRNA-MEND or Control-MEND (data not shown). In addition, εRNA-MEND has the specific effect on the replication of HBV, but not HCV in Huh-7.5 cells (Figure 6B). These data suggest that the results (Figures 6C and 6D) might not be mainly influenced by massive production of antiviral cytokines, although the cross-reactivity of cytokines should be still carefully considered. Therefore, it is presumed that the effect of εRNA might be based on not only its antagonistic activity but also its cytokine-inducing activity. These findings might afford a new therapeutic modality in replace of conventional antiviral drugs that have been reported to have a risk to develop drug-resistance HBV (Song et al., 2012). The present study might provide a better approach to the strategy for development of nucleic acid medicine and offer an attractive clinical option for the therapy against not only HBV but also possibly other virus infections.